Molecular dynamics simulation of liquid anisotropy. II. Rise and fall transients on a picosecond time scale

M. W. Evans

Chemistry Department, University College of Wales, Aberystwyth, Dyfed, SY23 1NE, Wales
(Received 7 April 1981; accepted 22 June 1981)

The behavior of a liquid sample subjected to an external torque of picosecond duration is investigated by molecular dynamics simulation, using 108 C_{2v} triatomics interacting with a 3×3 site–site Lennard-Jones potential. The resulting rise and fall transients are computed and their behavior is such as to fall on Langevin's functions from the linear response region to saturation, i.e., when the energetic perturbation (E) is less than kT to the point at which it is about 10 times kT. The breakdown of the fluctuation–dissipation theorem is investigated at the point $E/kT = 12$, where the normalized fall transients no longer decay as the equilibrium autocorrelation functions but considerably faster. The simulation does not support the conventional view of rise and fall transients, which is based on Debye's theory of rotational diffusion.

I. INTRODUCTION

In the second part of this series we extend our attention to rise and fall transients,[1] using a pulse of mechanical torque (Sec. II), picoseconds in duration. The anisotropy in the liquid is developed after a time lag, resulting in the characteristic time-dependent curves familiar[2] in experiments concerned with the induction of birefringence by various kinds of intense external fields. The magnitude of the external torque used in the simulation (Sec. II) is greater in energetic terms than the thermal kT, so that the fluctuation–dissipation theorem is no longer available analytically. This is investigated further in Sec. II of this paper. In Sec. III we define and illustrate the averages used to build up the various transients under investigation, and in Sec. IV pursue some of the implications.

II. COMPARISON OF TRANSIENT AND EQUILIBRIUM AVERAGES

Consider the return to equilibrium of a dynamical variable A after taking off at $t = 0$ the constant torque applied prior to this instant in time. If the torque is removed instantaneously, then the fluctuation–dissipation theorem[3] implies that the normalized fall transient will decay with the same time dependence as the autocorrelation function $\langle A(t)A(0)\rangle/\langle A(0)A(0)\rangle$. Therefore,

$$[\langle A(t)\rangle - A_{eq}]/[\langle A(0)\rangle - A_{eq}] = \langle A(t)A(0)\rangle/\langle A(0)A(0)\rangle \ , \qquad (1)$$

where A_{eq} is the equilibrium average value as $t \to \infty$ after the initial $t = 0$.

Theories are available linking the shape of the rise and fall transients which we can extract (Sec. III) from the simulation However, these are based on idealizations of the molecular dynamics[4] which are not supported by the results in part I of this series. If we use Bénoit's work on rotational diffusion, the decay transient is a pure exponential, which is not the case with the 108 C_{2v} molecules we have used in part I. Indeed, the results of Sec. III of this paper for our simple and purely mechanical externally applied torque $\mathbf{T}_{ext}$ (part I) are similar to those of Coelho and Manh,[2] who used experimentally Kerr effect relaxation for three chlorinated biphenyls at much lower frequencies than those pertinent to the work described here.

Equation (1), the fluctuation–dissipation theorem for a square pulse of external perturbation, is not applicable as we illustrate in Figs. 1 and 2 for the orientation vector $\mathbf{e}_B$. Plotted in Fig. 1 is the $\langle e_{BY}(t)\rangle$ (dotted line) fall transient after removal at $t = 0$ of the torque described in part I. The component e_{BY} of the vector $\mathbf{e}_B$ is the one affected by the torque [the transients $\langle e_{BX}(t)\rangle$ and $\langle e_{BZ}(t)\rangle$ are about 1% of $\langle e_{BY}\rangle$ in absolute magnitude]. According to Eq. (1), $\langle \mathbf{e}_B(t)\rangle/\langle \mathbf{e}_B(0)\rangle$ should be the same as $\langle \mathbf{e}_B(t)\cdot\mathbf{e}_B(0)\rangle/\langle \mathbf{e}_B(0)\cdot\mathbf{e}_B(0)\rangle$ in the absence of any perturbation, but actually decays more quickly. Note that the transient as computed here is an average over 108 molecules. However, from Figs. 8 and 9 this is clearly equivalent to taking the usual *single molecule* thermodynamic average in the limit $t \to \infty$ of the transient. It is therefore valid to compare these transients with *auto*correlation functions at equilibrium. Similarly, if we construct the transient average

$$\langle 3[\mathbf{e}_B(t)\cdot\mathbf{e}_B(t)] - 1\rangle/\langle 3[\mathbf{e}_B(0)\cdot\mathbf{e}_B(0)] - 1\rangle$$

and compare this with the equilibrium autocorrelation function

$$\langle 3[\mathbf{e}_B(t)\cdot\mathbf{e}_B(0)]^2 - 1\rangle/\langle 3[\mathbf{e}_B(0)\cdot\mathbf{e}_B(0)]^2 - 1\rangle \ ,$$

the former again decays more quickly (Fig. 2), although

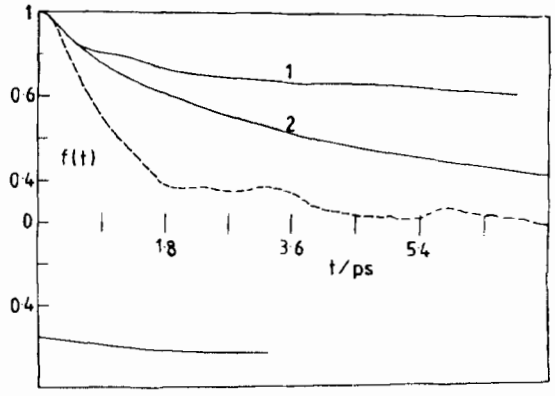

FIG. 1. Comparison of $\langle P_1\rangle$ normalized orientational autocorrelation functions (—) and normalized fall transients (----) for an external torque of saturation strength ($\mu F/kT = 12$ in energetic terms): (1) torque-on case, (2) torque-off case, ---, Fall transient.

 0021-9606/82/115480-04$02.10

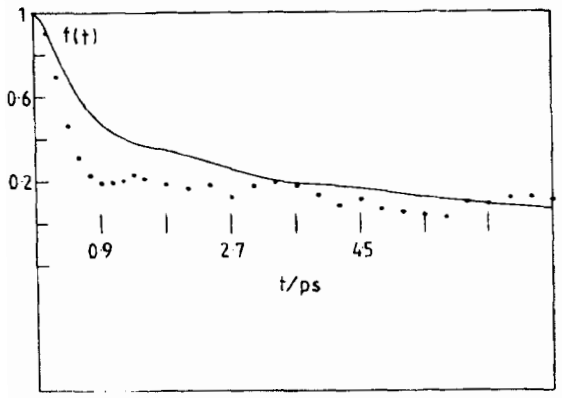

FIG. 2. —, $\langle P_2 \rangle$ normalized orientational acf, torque-off case. •, Normalized fall transient for P_2.

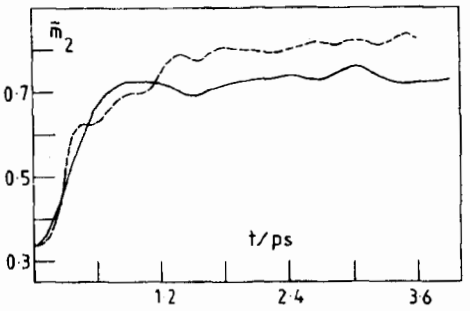

FIG. 4. Rise transient (—) and mirror image of fall transient (----) for the case $\bar{m}_2 = \langle e_{BY}^2 \rangle$ in the saturation regime $\mu F/kT = 12$. The mirror image of the fall transient is constructed by superimposing the fall transient (dashed line) on the rise transient in such a way that $\bar{m}_2$ at $t = 0$ is the same for both functions, i.e., we have "held a mirror" to the rise transient.

the time scales are more similar. This is the first problem therefore to be tackled by the analytical approach, and is a fundamental hurdle to overcome when dealing with data from electro-optical techniques using intense external fields. Examples are pulsed high field dielectric transient measurements,[5] Kerr effect measurements, etc. The molecular dynamics simulation used here is intended only as a guide (see part I) but simulations on real systems are feasible with the computer power now available. The so-called nonlinear response theory can then be put to the test using molecular dynamics simulation. It is clear from the present results that the statistics of the analytical theory should be *non*-Markovian, unlike the great majority of the previous attempts to analyze rise and fall transients of this nature[4] (e.g., Benoit, Ullman, and others).

III. RELATIVE TIME SCALES OF THE TRANSIENTS

The analytical knowledge in this area is based on modeling with relatively unrealistic concepts. The results are expressed essentially as averages of the type $\langle A^n \rangle$, where A is a dynamical vector, usually an orientation axis such as $\mathbf{e}_B$ embedded in the molecule and defined with respect to the laboratory frame. Using models, the relationship between these averages may be derived for positive integral n. It is more straightforward to work with fall transients in this context.[6]

The computer simulation allows us to calculate $\langle e_{BY}^n \rangle$ rise and fall transients, and in this section we illustrate the results up to $n = 6$.

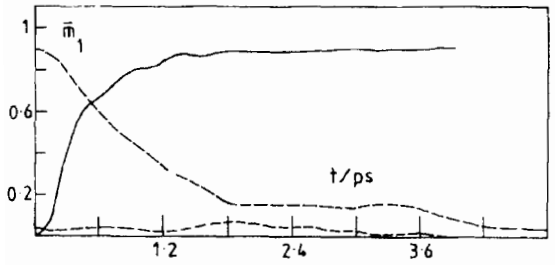

FIG. 3. Rise and fall transients $\bar{m}_1 = \langle e_{BY} \rangle$ in the saturation regime, $\mu F/kT = 12$. —, Rise transient; ---, fall transient.

In Fig. 3 the rise and fall transients for $\langle e_{BY}(t) \rangle$ itself are clearly not contemporaneous, the fall transient being the longer lived, and, in common with the equilibrium acf of $\mathbf{e}_B$ (Fig. 1), nonexponential. Note that because the simulation is carried out on a microcanonical ensemble, the fall transient in Fig. 3 must be accompanied by a temperature change, but this is countered in the simulation by thermostating to a constant temperature, if necessary, every 50 time steps. The autocorrelation function is computed using a running time average at this same temperature and is therefore directly comparable with the transients. The inputted temperature is 220 K. In addition to the thermal energy there is of course a dipole interaction energy. The transient curves are not as smooth as the acf's because in the former case $\langle\ \rangle$ means an average over the 108 molecules only, and in the latter a running time average in the usual way.[7] Therefore, the short-time oscillation in the rise transient and the plateau from 1.8 to 3.6 ps in the fall transient may be different for different square-wave amplitude and duration. The fall transient is established after only 1.8 ps, reflecting the intense $\mathbf{T}_{ext}$ used (part I).

The transient averages $\langle e_{BY}^2 \rangle$ are plotted in Fig 4. The

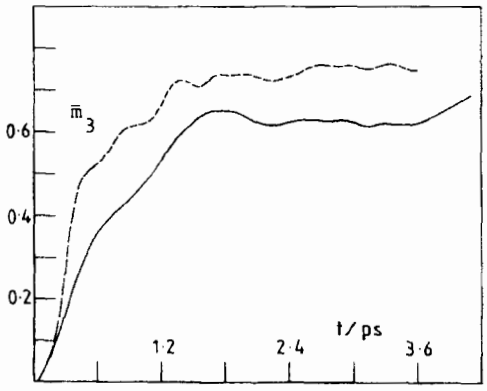

FIG. 5. Rise transient (—) and mirror image of fall transient (----) for the case $\bar{m}_3 = \langle e_{BY}^3 \rangle$ in the saturation regime $\mu F/kT = 12$.

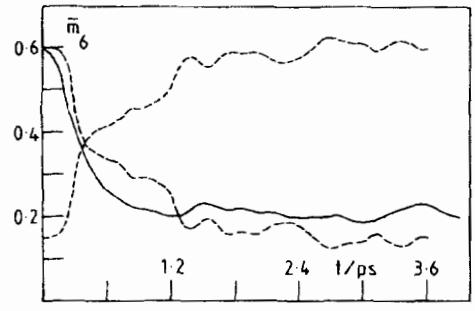

FIG. 6. Rise transients (----) and fall transients (—) for $\bar{m}_6 = \langle e^6_{BY} \rangle$ in the saturation regime $\mu F/kT = 12$.

rise transient is faster again in this case. The fall transient does not reach the "no-order" level of $\frac{1}{3}$ in 8.0 ps. The behavior of $\langle e^3_{BY} \rangle$ in Fig. 5 is similar, and this continues to be the case up to $\langle e^6_{BY} \rangle$ (Fig. 6). The rise transients are plotted together for comparison in Fig. 7, and are essentially contemporaneous, for the mechanical torque T_{ext} applied in the simulation.

IV. DISCUSSION

The simulated transients in Sec. II and III are only simulations, i.e., the product of an elaborate theoretical exercise. Nevertheless, in pursuing the implications it is interesting to refer to such data as are available. Those of Coelho and Manh[2] are particularly interesting in this context despite the fact that they refer to a much longer time scale than used in the simulation and were obtained with Kerr effect and dielectric methods, i.e., with an electrically applied external torque. Their observed relaxation times/Kerr effect decay transients are *similar* over a wide range of temperature for each of the systems studied. Rise and decay transients for tritolyl phosphate[2] are both governed by the same relaxation function, i.e., this takes the form $[1 - \alpha(t)]$ for the rise transient and $\alpha(t)$ for the decay. They are contemporaneous. In the simulation this appears to be more nearly the case for $\langle e^2_{BY} \rangle$ than for $\langle e_{BY} \rangle$ itself. The major difference between the simulation and the results of Coelho and Manh is that we can apply a stronger perturbation than is possible experimentally with electric fields, even when pulsed. The major experimental features of Coelho and Manh are however similar to the simulation results.

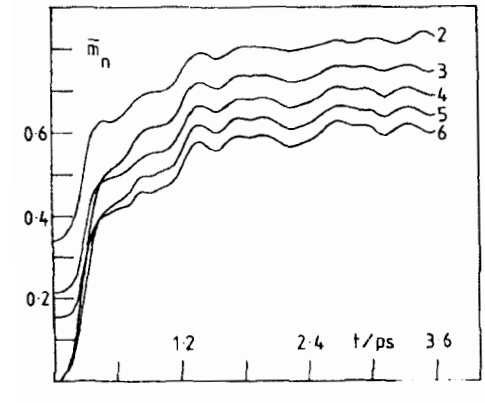

FIG. 7. Rise transients $\bar{m}_n$ in the case $n = 2$ to $n = 6$.

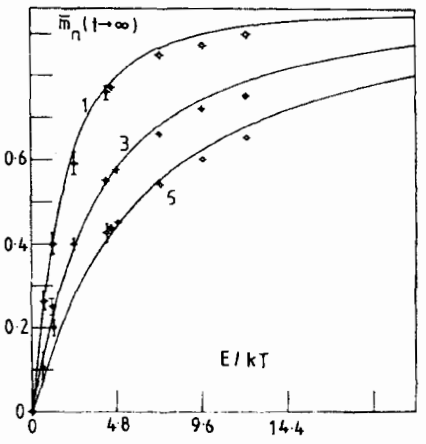

FIG. 8. Langevin functions vs $\mu F/kT$ from the linear response regime to the saturation regime; $\bar{m}_n(t \to \infty)$ for $n = 1, 3, 5$. ◇, Points taken from the computer simulation. —, Theoretical curves, calculated using Boltzmann statistics (see Appendix A). The points ◇ are fitted to — using a nonlinear least mean squares best fit.

With advances in simulation technique, computer availability, and power, it is feasible to attempt in the near future a simulation of the ps Kerr effect or high field dielectric data now becoming available. This would mean using polarizable molecular potentials to consider interactions which are nonlinear in the applied electric field.

V. LANGEVIN'S FUNCTION

In Fig. 8 is plotted the graph of $\langle e_{BY} \rangle_{t \to \infty}$ against E/kT, where E is the perturbation energy. By $\langle e_{BY} \rangle_{t \to \infty}$ we mean the level finally attained by the average $\langle e_{BY} \rangle$ in the torque-on case. By reference to Appendix A we have the theoretical result that $\langle e_{BY} \rangle_{t \to \infty}$ should follow Langevin's function $L(\mu F/kT)$, where μF is the effective me-

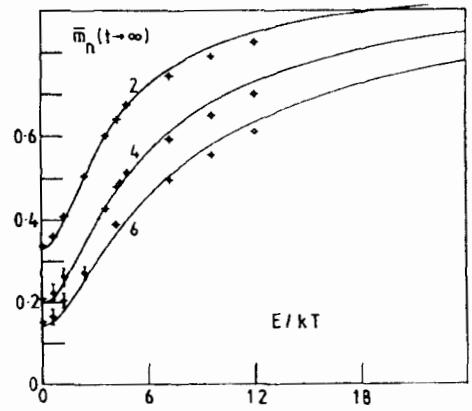

FIG. 9. As for Fig. 8, $n = 2, 4, 6$. In the case $\mu F/kT \to 0$ we have $\bar{m}_2(t \to 0) = 1/3$ theoretically compared with a simulation result of 0.34. In addition, $\bar{m}_4(t \to 0) = 1/5$, compared with 0.210, and $\bar{m}_6(t \to 0) = 1/7$, compared with 0.150.

chanical energy due to the applied torque and kT the mean thermal energy. In Fig. 8 we have fitted the simulation results for $\langle e_{BY}\rangle_{t\to\infty}$ to a form $L(a)$, where a is allowed to vary. The numerical routine was based on a nonlinear least mean squares algorithm. The best fit is illustrated in Fig. 8 with energy ratios $\mu F/kT$ plotted along the abscissa. The theoretical higher order Langevin functions for $\langle e^n_{BY}\rangle_{t\to\infty}$ are derived in Appendix A and least mean squares fitting exercises for $\langle e^n_{BY}\rangle_{t\to\infty}$ should provide the same value of a provided the simulation results are accurately the same as those expected theoretically. With the nonlinear least mean square fitting routine used, this is indeed found to be the case (Figs. 8 and 9).

These results therefore prove that it is possible to reproduce Langevin's function, and the associated higher order functions, with molecular dynamics simulation, from the linear response regime to the saturation regime. The advantage of doing this in theoretical terms is that models of nonlinear response and equations of the Kramers type[4,6] can be tested out against the computer results, and predictions, made up of the effect of saturating fields on any acf of interest.

ACKNOWLEDGMENT

The S. R. C. is acknowledged for financial support.

APPENDIX A: THE LANGEVIN INTEGRALS

Denote the mean level of $\langle e^n_{BY}\rangle$ as $t\to\infty$ by $\bar{m}_n$. Using Boltzmann statistics, we have

$$\bar{m}_n = \mu \frac{\int_{-1}^{1} e^{ax} x^n\, dx}{\int_{-1}^{1} e^{ax}\, dx} \quad , \tag{A1}$$

where $a = \mu F/kT$ is the ratio of the effective mean coupling energy in the system to the thermal energy (kT). In our case μF is the mechanical energy, μ being its effective arm and $\mathbf{F}$ the external force. In our case further $|\boldsymbol{\mu}| = |\mathbf{e}_B| = 1$. Therefore, working out the integrals in Eq. (A1) gives

$$\bar{m}_n = \left(\frac{a}{e^a - e^{-a}}\right)\left[e^{ax}\sum_{r=0}^{m}(-1)^r \frac{m!\, x^{m-r}}{(m-r)!\, a^{r+1}}\right]_{-1}^{1} . \tag{A2}$$

From Eq. (A2),

$$\bar{m}_1 = \frac{e^a + e^{-a}}{e^a - e^{-a}} - \frac{1}{a} \equiv L(a) \quad , \tag{A3}$$

where $L(a)$ is the Langevin function.

Further,

$$\begin{aligned}\bar{m}_2 = \langle e^2_{BY}\rangle &= 1 - \frac{2}{a}L(a) \\ &= 1 - \frac{2}{a}\left(\frac{a}{3} - \frac{a^3}{45} + \cdots\right) \\ &\to \tfrac{1}{3} \text{ as } a \to 0 \ .\end{aligned} \tag{A4}$$

(The molecular dynamics simulation produces $\langle e^2_{BY}\rangle = 0.34$ in the absence of an externally applied force.)

The next integral is

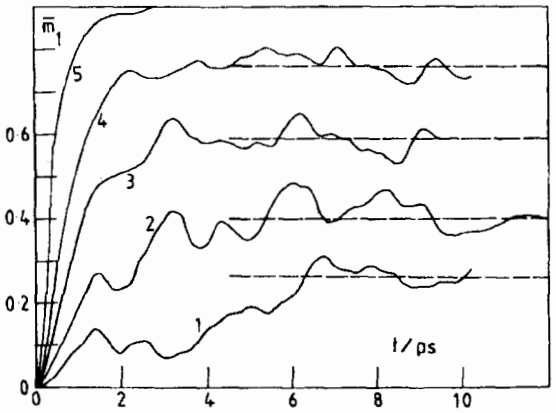

FIG. 10. Comparison of rise transients $\langle e_{BY}\rangle$ for different $\mu F/kT$. (1) $\mu F/kT = 0.6$; (2) 1.2; (3) 2.4; (4) 4.2; (5) 12.0.

$$\bar{m}_3 = \langle e^3_{BY}\rangle = \frac{e^a + e^{-a}}{e^a - e^{-a}} - \frac{3}{a}\bar{m}_2 \ . \tag{A5}$$

Higher $\bar{m}_n$ are easily evaluated using the relation

$$\int e^{ax} x^m\, dx = \frac{x^m e^{ax}}{a} - \frac{m}{a}\int e^{ax} x^{m-1}\, dx \ . \tag{A6}$$

This provides us with

$$\bar{m}_4 = 1 - \frac{4}{a}\bar{m}_3 - \frac{1}{5} \quad \text{as } a \to 0 \ , \tag{A7}$$

$$\bar{m}_5 = \frac{e^a + e^{-a}}{e^a - e^{-a}} - \frac{5}{a}\bar{m}_4 \ , \tag{A8}$$

$$\bar{m}_6 = 1 - \frac{6}{a}\bar{m}_5 - \frac{1}{7} \quad \text{as } a \to 0 \ , \tag{A9}$$

and so on.

APPENDIX B

In this Appendix we illustrate the method of obtaining the simulated Langevin functions of Figs. 8 and 9 by reference to Fig. 10. The slashed lines refer to the average level as $t\to\infty$. Note that as E increases the rise time of each transient decreases, and the noise level in $\bar{m}_n$ also decreases. It is not possible to reproduce these curves easily with the fluctuation–dissipation theorem and linear response theory. The rise transients are always "field-on" phenomena.

[1] C. J. F. Bottcher and P. Bordewijk, *Theory of Electric Polarisation* (Elsevier, Amsterdam, 1978).
[2] R. Coelho and Do Khac Manh, C. R. Acad. Sci. Ser. C 264, 641 (1967).
[3] M. W. Evans, A. R. Davies, and G. J. Evans, Adv. Chem. Phys. 44, 255 (1980).
[4] H. Bénoit, J. Chim. Phys. 49, 517 (1952); R. Ullman, J. Chem. Phys. 56, 1869 (1972).
[5] *Dielectric and Related Molecular Processes*, edited by M. Davies (The Chemical Society, London, 1975), Vol. 2.
[6] M. W. Evans, W. T. Coffey, P. Grigolini, and G. J. Evans, *Molecular Dynamics* (Wiley/Interscience, New York, in press), Chaps. 9 and 10.
[7] Reference 6, Chap. 1.